Electrooxidation of Formamidine Disulfide Simultaneously Investigated by On-Line High Performance Liquid Chromatography and Cyclic Voltammetry

Wei Zhang,*[a] Hainan Luo,[a] Fengli Li,[a] Baoying Zhang,[a] Yuyan Zhao,[a] Na Feng,[b] and Yang Liu*[a]

The electro-oxidation of formamidine disulfide, an important sulfur-containing compound, was simultaneously investigated with on-line high-performance liquid chromatography and cyclic voltammetry. Using a home-made microporous sampler located at the electrode interface, the solution on the electrode surface was in situ sampled and analyzed. The electrochemical scanning was synchronously performed, which allowed the electro-oxidation products to be detected at a given potential. The main products on the surface of platinum electrode were found to be thiourea, formamidine sulfinic acid, cyanamide, and elemental sulfur. Forced convection arising from the sampling played an important role in the electrochemical oxidation. The extraction of electrode surface solution promoted the renewal of reactant and its intermediates, which induced the change of cyclic voltammetry curve. The forced convection also contributed to the redox peak current of the species on the cyclic voltammetry curves through the change of concentration of reactant and its intermediates. This technique can help to explore the reaction mechanism of complex electrochemical reactions.

1. Introduction

Formamidine disulfide ($[(NH_2)_2CS\text{-}SC(NH_2)_2]^{2+}$ or TU_2^{2+}) is widely used in medicines, pesticides, metal plate etching, and anticorrosion.[1] It is also found to be an important product of electrochemical oxidation of thiourea (TU).[2–5] A variety of studies have shown that abundant nonlinear dynamical phenomena occur in the TU oxidation process.[6–9] As an intermediate of such processes, the TU_2^{2+} exhibits different valence changes and various products, including oxides and free radicals, as well as the occurrence of autocatalytic and hydrolysis reactions.[10–11]

A. E. Bolzán et al. applied voltammetry and rotating ring-disk electrode techniques to study electrochemical response of thiourea and formamidine disulphide on polycrystalline platinum electrode. The electro-oxidation of thiourea on platinum involves two stages occurring in different potential windows, yielding soluble formamidine disulphide as the main product.[12]

Gabriela studied the oxidation of thiourea and TU_2^{2+} on polycrystalline platinum electrode using in situ Fourier transform infrared spectroscopy (FTIRS) and different electrochemical mass spectrometry (DEMS).[13] A dual-path reaction mechanism was proposed. The first step was initialed from dissolved TU at $E > 0.55\ V_{RHE}$. The produced TU_2^{2+} was then oxidized to soluble NH_2CN at $E > 1.30\ V_{RHE}$. The second parallel reaction occurred from adsorbed TU at $E > 0.60\ V_{RHE}$ and implied the formation of adsorbed species, i.e., NH_2CN, SCN and S.

The thiourea and TU_2^{2+} on gold electrode were also studied by combining density functional theory (DFT) calculations with external reflection infrared spectroscopy and surface-enhanced infrared reflection-absorption spectroscopy under attenuated total reflection conditions (ATR-SEIRAS).[14] The optimized geometry was obtained from DFT calculations. Then the experiments were performed on the adsorbed TU to unidentate bonding through the sulfur atom, with the Au–S bond slightly tilted (13 degrees) from the surface normal.

Previous studies on the thiourea or TU_2^{2+} oxidation system mainly relied on the methods of chemical titration. However, the titration shows obvious limitations, such as the complexity of the product and the possibility of continuing homogeneous chemical reaction. The inaccurate titration of some products of low concentration may also cause the negligence of time-resolved products. Meanwhile the electrochemical analysis lacks a clear electrochemical / optical fingerprint spectrum in the analysis of ionic reaction products. Moreover, the electrode products cannot be measured quantitatively. The on-line high-performance liquid chromatography (HPLC) combined voltammetry technique provides a novel way to determine the electrode intermediates involved in electrochemical reactions at

[a] Dr. W. Zhang, Dr. H. Luo, Dr. F. Li, B. Zhang, Y. Zhao, Dr. Y. Liu
College of Chemistry, Chemical Engineering and Materials Science
Zaozhuang University
Zaozhuang (China)
E-mail: zhangwzlj@163.com
chemliuyang@uzz.edu.cn
[b] N. Feng
College of Chemical Engineering
Yangzhou Polytechnic Institute
Yangzhou (China)

Supporting information for this article is available on the WWW under https://doi.org/10.1002/open.202100197 https://doi.org/10.1002/open.202100197

a given potential.[9,15–17] Now this method is typically used for online detection of the species and concentration changes on the electrode surface. As shown in Figure 1, a micro-sized sample collection tip (inner diameter of 0.3 mm) was fixed on the surface of the working electrode. A small amount of solution was collected from the surface of the electrode by a peristaltic pump, and then the sample was analyzed by a HPLC. During the sampling, forced convection was generated by the extraction of liquid at the electrode surface. The rate of forced convection was directly related to the speed of peristaltic pump. The convective mass transfer process proceeded from the edge of the electrode to the center of the disk, as shown in Figure 1. Obviously, a faster sampling rate of the peristaltic pump produces a stronger forced mass transfer process as well as faster renewal of the material on the surface of the electrode. Similar methods of the forced mass transfer on the electrode surface are rotating disk electrode (RDE) and rotating ring-disk electrode (RRDE), whereas the mass transfer direction with RDE or RRDE proceeds from the center of the disk to the edge, as shown in Figure 2. RRDE are widely used in the study of electrode reactions and electrochemical analysis.[18–19] It was found that the mass transfer processes on the surface of a RDE or RRDE were affected by the rotation of the electrode, where the diffusion of the electrode products was proportional to the rotation speed. Owing to the high-speed rotation of the disk electrode, the solution near the surface of the disk was rapidly thrown to the edge under the action of centrifugal force. The soluble reaction products and intermediates quickly migrated to the ring electrode. The generation of an electrode intermediate is determined by applying a potential on the electrode ring. RRDE includes speed control device and two sets of potentiometers connected with disk electrode and ring electrode respectively, whereas our applied procedure only inlcude a sampler on the electrode surface and a peristaltic pump to determine the generation of electrode intermediates. Compared with RRDE, our applied procedure has great advantages in both cost and efficiency in determining electrode intermediates (for a comparison table for applied procedure with other methods (see Table S1 and S2 in the Supporting Information).

In this study, we use on-line HPLC combined cyclic voltammetry to study the electrochemical oxidation of TU_2^{2+}. The relationship between the distribution of electrode products and electrode potential can be obtained qualitatively and quantitatively by using the combined technique. By using a home-made microporous sampler located at the electrode interface, the solution on the electrode surface was in situ sampled and analyzed. Forced convection arising from the sampling played an important role in the electrochemical oxidation. The forced convection also contributed to the redox peak current of the species on the cyclic voltammetry curves through the change of concentration of reactant and its intermediates. This method is helpful to explore the kinetics and mechanism on the electrode surface reactions.

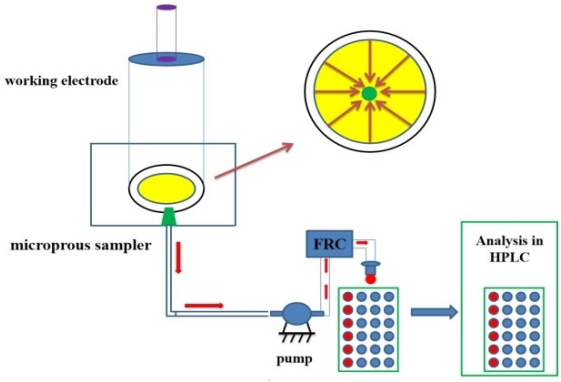

Figure 1. Scheme of the on-line HPLC combined Voltammetry technique.

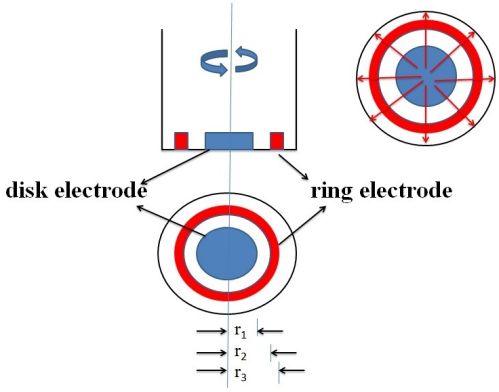

Figure 2. Scheme of the rotating ring-disk electrode.

2. Results and Discussion

To study the effect of parameters of TU_2^{2+}, the effect of the scan rate on the peak current were investigated. Figure 3 presents the influence of the scan rate on the electro-oxidation of TU_2^{2+} on the platinum electrode. In the potential range of −0.1 to 0.8 V, an anodic peak was observed during the forward scan, which was corresponding to the oxidation of TU, the electrode reduction product of TU_2^{2+}. During the reverse scan, a cathodic peak was observed, corresponding to the reduction peak of TU_2^{2+}, the reduction product of which was TU, as shown

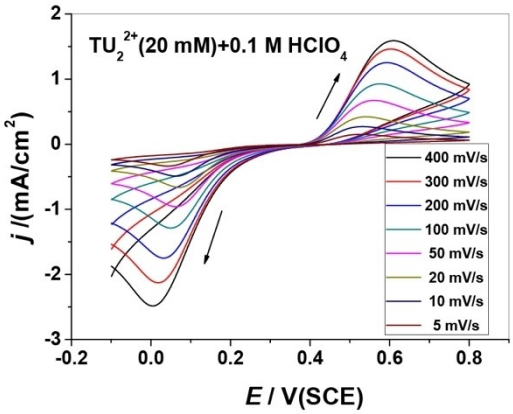

Figure 3. Cyclic voltammograms of TU_2^{2+} at various scanning rates. Conditions: $[TU_2^{2+}] = 0.02$ M, $[HClO_4] = 0.1$ M, and $T = 25.0 \pm 0.1$ °C.

in equation (R1) and (R2). Figure 4 shows the relation between the peak current and the sweep speed for TU_2^{2+}. The peak currents of the anodic oxidation peak and cathodic reduction peak of TU_2^{2+} were linearly related to the square root of the sweep speed. Therefore, the oxidation and reduction of TU_2^{2+} were diffusion-controlled processes.

$$2(NH_2)_2CS - 2e^- \rightarrow [(NH_2)_2CSSC(NH_2)_2]^{2+} \quad (R1)$$

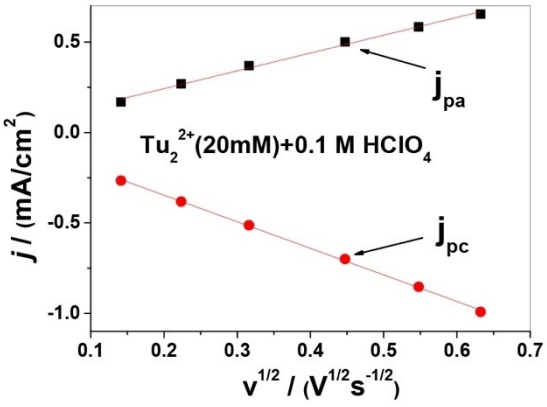

Figure 4. Plot of j_p *vs.* $v^{1/2}$ for TU_2^{2+}. Conditions: $[TU_2^{2+}] = 0.02$ M, $[HClO_4] = 0.1$ M, and $T = 25.0 \pm 0.1$ °C.

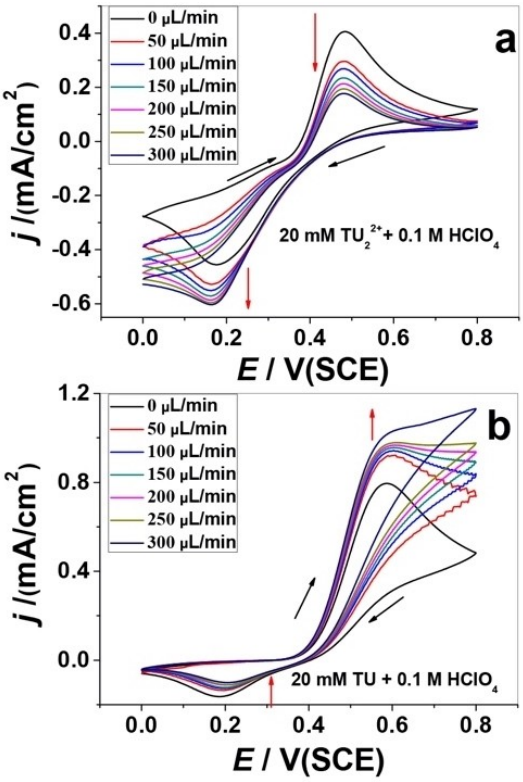

Figure 5. Cyclic voltammograms of (a) TU_2^{2+} and (b) TU at various sampling rates. The black arrow indicates the scanning direction, and the red arrow indicates the direction in which the peak current changes with the sampling rate. Conditions: $[TU_2^{2+}] = 0.02$ M (a), $[TU] = 0.02$ M (b), $[HClO_4] = 0.1$ M, scanning rate = 10 mV s^{-1}, and $T = 25.0 \pm 0.1$ °C.

$$[(NH_2)_2CSSC(NH_2)_2]^{2+} + 2e^- \rightarrow 2(NH_2)_2CS \quad (R2)$$

The main oxidation product of TU was TU_2^{2+} while the TU_2^{2+} can be reduced to TU, which made a reversible redox reaction. The effects of sampling on the electro-oxidation of TU_2^{2+} and TU in the range of 0 V to 0.8 V were investigated separately. The forced convection at the electrode interface generated completely different effects on the cyclic voltammetry curves of TU and TU_2^{2+}. Figure 5a shows the cyclic voltammograms of TU_2^{2+} at various sampling rates. As the sampling rate increases, the current density of the cathodic peak (0.16 V) increases gradually, whereas the current density of the anodic peak (0.48 V) decreases gradually. Figure 5b shows the cyclic voltammograms of TU at various sampling rates. An increase of the sampling rate on the electrode surface leads to a gradual decrease of the cathodic peak current (0.18 V) with a simultaneous gradual increase of the anodic peak current (0.58 V).

From the change of the cathodic peak in figure 5a and the oxidation peak in Figure 5b, it appears that the species in solution participated in the electrochemical reaction. The sampling accelerated the mass transfer and generated a larger current. The change of the cathodic peak in Figure 5b and the oxidation peak in Figure5a indicated that sampling induced the decrease of concentration of the electrode intermediates on the electrode surface when the intermediates continued to be involved in the electrochemical reaction. Thus, the peak current would be eventually decreased. Based on these characteristics, it is possible to determine whether the species in solution or the electrode intermediates are involved in the reaction. The liquid-pumping is similar to the RRDE method, which both can detect the intermediate products on the electrode. The difference is that the current process in liquid-pumping is much simpler than the RRDE.

In the solution of TU_2^{2+}, there was a current oscillation during the reverse scan in the potential range of 0–0.1 V, as shown in Figure 5a. TU_2^{2+} was reduced to TU in this potential range. The oscillation frequency was increased with a higher sampling rate. In the solution of TU, there was also a current oscillation in the range of 0.6–0.8 V during sampling, as shown in Figure 5b. In this potential range, TU was oxidized to TU_2^{2+}, and the oscillation frequency was increased while the sampling rate was elevated.

The linear voltammograms of TU_2^{2+} and TU are shown in Figure 6. With the increase in sampling rate, the reduction peak current of TU_2^{2+} was gradually increased and finally reached a plateau. Similar behavior was observed for the oxidation peak current of TU. These phenomena were similar to the electro-oxidation of thiosulfate, thiourea and formamidine disulphide observed on RDE, the oxidation peaks reach a plateau as the increase of rotation speed of rotating disk electrode increases.[12,20]

Cyclic voltammograms of TU_2^{2+} were investigated in the range of −0.2 to 1.6 V, as shown in Figure 7. There were three regions in the cyclic voltammetry curve of TU_2^{2+}, i.e., region A, B, and C, which were obviously affected by forced convection.

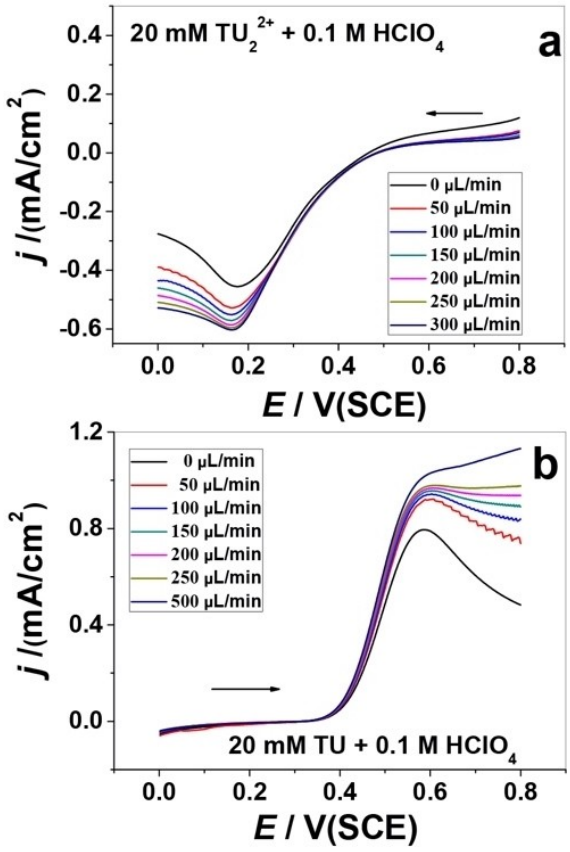

Figure 6. Linear voltammograms of (a) TU_2^{2+} and (b) TU at various sampling rates. Conditions: $[TU_2^{2+}] = 0.02$ M (a), $[TU] = 0.02$ M (b), $[HClO_4] = 0.1$ M, scanning rate = 10 mV s^{-1}, and T = 25.0 ± 0.1 °C.

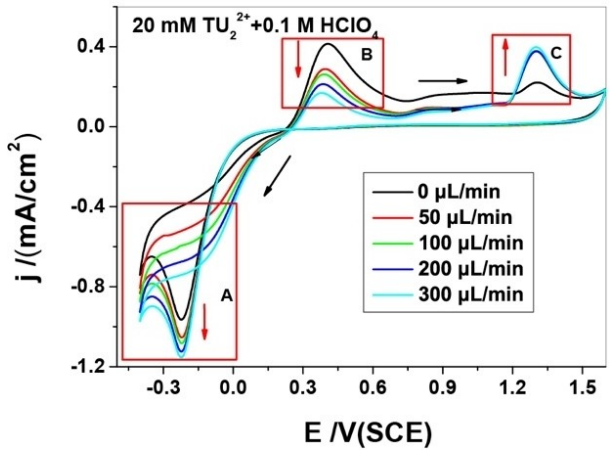

Figure 7. Cyclic voltammograms of TU_2^{2+} in the range of −0.4 to 1.6 V at various sampling rates. The black arrow indicates the scanning direction, and the red arrow indicates the direction in which the peak current changes with the sampling rate. Conditions: $[TU_2^{2+}] = 0.01$ M, $[HClO_4] = 0.1$ M, scanning rate = 10 mV s^{-1}, and T = 25.0 ± 0.1 °C.

As the sampling rate was increased, the current of the oxidation peak in region B was decreased at about 0.5 V, whereas the current of the oxidation peak in region C (~1.3 V)) was increased and the current of reduction peak in region (−0.3 V) was increased. The decrease of the current in region B indicated that an intermediate product was formed simultaneously. As the sampling rate was increased, a decrease in the amount of this intermediate product led to a decrease in the current. Based on the previous studies,[17] it was assumed that TU can be oxidized to formamidine sulfinic acid (TUO_2). The second oxidation peak current in region C was induced by the increase of the sampling rate. In combination with HPCL data shown in Figure8, this peak corresponded with the oxidation of TU_2^{2+} to TUO_2.

To avoid the interference of TU formation on electrode surface, a potential interval of 0.4–1.6 V was chosen to study the electrochemical oxidation of TU_2^{2+}, as shown in Figure 8. There was an oxidation peak at 1.3 V on the cyclic voltammetry curve of TU_2^{2+}, which proved that the oxidation peak at 1.3 V (in Figure 7) originated from the oxidation of TU_2^{2+}.

The first two cycles of cyclic voltammetry of TU_2^{2+} between potential of 0.5–1.6 V were plotted as shown in Figure 9. In the first lap of 1.3 V, the peak current was much larger than the peak current in the second lap. This indicated that the active site of the electrode surface was occupied by the oxidation products of TU_2^{2+}. These substances were electrochemical inert or lower electrochemical activity than TU_2^{2+}, hindering the

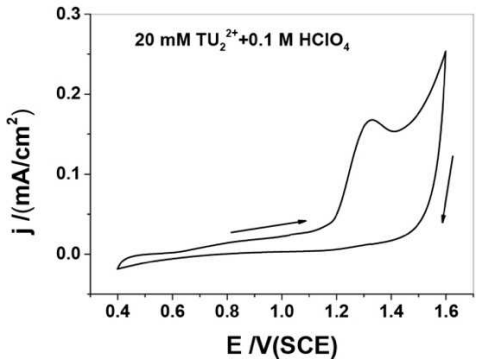

Figure 8. Cyclic voltammograms of TU_2^{2+} in the range of 0.4 to 1.6 V. Conditions: $[TU_2^{2+}] = 0.02$ M, $[HClO_4] = 0.1$ M, scanning rate = 10 mV s^{-1}, and T = 25.0 ± 0.1 °C.

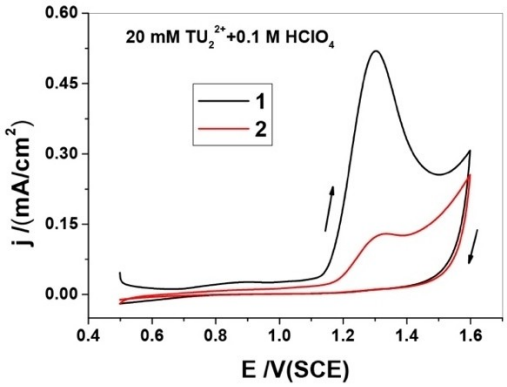

Figure 9. Cyclic voltammograms of TU_2^{2+} for the first two cycles in the range of 0.5 to 1.6 V. The black curve represents the first circle, the red curve represents the second circle. Conditions: $[TU_2^{2+}] = 0.02$ M, $[HClO_4] = 0.1$ M, scanning rate = 10 mV s^{-1}, and T = 25.0 ± 0.1 °C.

adsorption of TU_2^{2+} on the electrode surface. Thus, the oxidation peak current decreases eventually.

It can be seen from Figure 10a that there was only one oxidation peak at 1.3 V and the oxidation peak current was increased gradually with the negative shift of the starting potential of the potential scan. The lower starting scanning potential produced a greater the cathodic current when the potential was reversed. The surface of the electrode was cleaned due to the desorption or reduction of adsorbed substances on the surface of the electrode, so the oxidation peak current at 1.3 V was increased gradually. As shown in figure 10b, when starting potential of the potential scan was between 0.0–0.3 V, the oxidation peak current at 1.3 V decreases with the negative shift of the potential scan start potential. The oxidation peak current at 0.4 V was increased while the current platform in the range of 0.7–1.0 moved up. With the negative shift of the potential, the cathodic reduction peak gradually appeared and the TU_2^{2+} was reduced to TU. The adsorption amount of TU on the electrode surface was increased gradually with the negative shift of potential. The oxidation peak at 0.4 V was derived from the oxidation of thiourea. The decrease of oxidation peak current at 1.3 V indicated that a passivation layer is formed on the electrode surface, and the current between 0.7–1.0 V was increased with the increase of oxidation peak current at 0.4 V, which indicated that the passivation layer comes from thiourea, and there was sulfur deposition visible to the naked eye after scanning for more than 50 cycles.[21] Therefore, it was speculated that the passivation layer was mainly sulfur deposition, as shown in equation (R11).

The cyclic voltammetry combined with on-line HPLC was used to analyze the distribution and concentration of species on the working electrode surface. In Figure 11, the cyclic voltammogram of the electro-oxidation of TU_2^{2+} was obtained during electrode interface sampling in the potential range of 0–1.6 V. Three oxidation at 0.6, 1.0, and 1.3 V were observed during the forward scan. The samples collected during this process were then analyzed by HPLC. Data of liquid phase samples collected at different potentials were shown in Figure 12 and Figure 13. Three chromatographic peaks were observed during both the forward and reverse scans, as shown in Figure 12a and Figure 12b. The peaks at retention times of

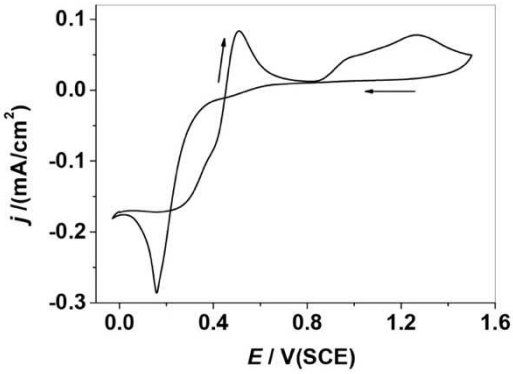

Figure 11. Cyclic voltammogram for the electro-oxidation of TU_2^{2+} during electrode interface sampling. Conditions: $[TU_2^{2+}] = 0.02$ M, $[HClO_4] = 0.1$ M, scanning rate = 1 mV s^{-1}, sampling rate = 60 μL min^{-1}, and T = 25.0 ± 0.1 °C.

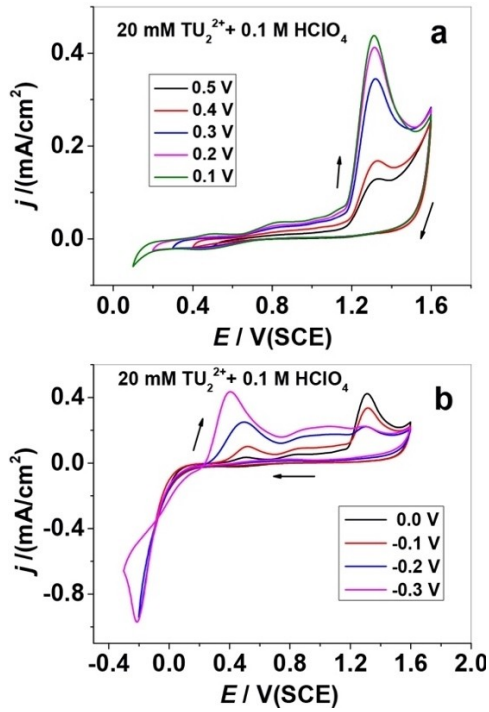

Figure 10. Cyclic voltammograms of TU_2^{2+} at different scan start potential. (a) The scan onset potential decreased gradually 0.5 V to 0.1 V. (b) The scan onset potential decreased gradually 0.0 V to −0.3 V. Conditions: $[TU_2^{2+}] = 0.02$ M, $[HClO_4] = 0.1$ M, scanning rate = 10 mV s^{-1}, and T = 25.0 ± 0.1 °C.

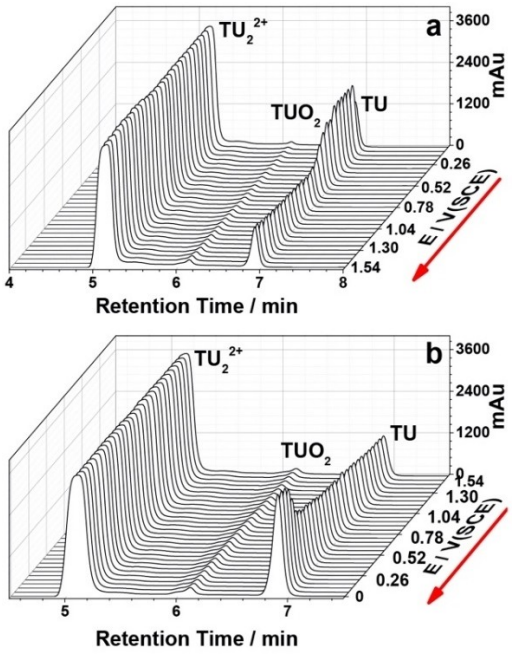

Figure 12. HPLC chromatograms for the oxidation of TU_2^{2+} at various potentials on the Pt electrode: (a) forward scan and (b) reverse scan. Conditions: $[TU_2^{2+}] = 0.02$ M, $[HClO_4] = 0.1$ M, scanning rate = 1 mV s^{-1}, sampling rate = 60 μL min^{-1}, and T = 25.0 ± 0.1 °C.

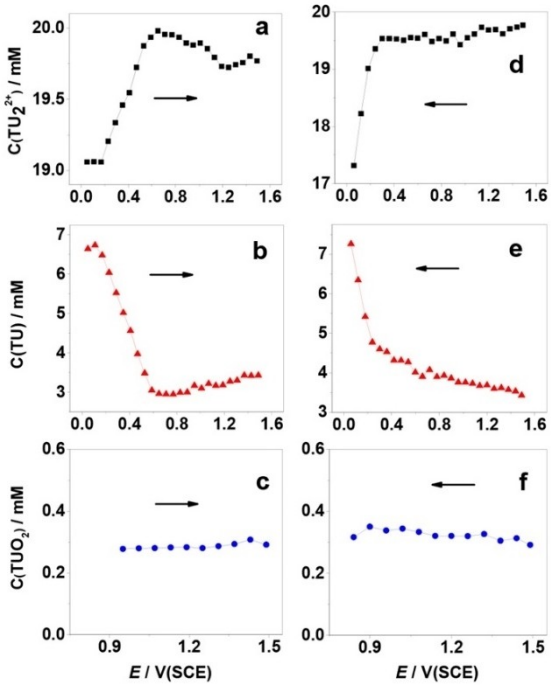

Figure 13. Concentrations of TU_2^{2+} (a, d) and its electro-oxidation by-products, TU (b, e) and TUO_2 (c, f), as functions of time on the Pt electrode: (a–c) forward scan and (d–f) reverse scan. Conditions: $[TU_2^{2+}] = 0.02$ M, $[HClO_4] = 0.1$ M, scanning rate = 1 mV s^{-1}, sampling rate = 60 μL min^{-1}, and T = 25.0 ± 0.1 °C.

6.88, 6.18, and 4.97 min were corresponding to TU, TUO_2, and TU_2^{2+}, respectively. As the peak areas represented the concentrations of these species, it was possible to determine the species on the electrode surface both qualitatively and quantitatively as a function of the electrode potential.

A series of in situ surface sensitive technologies has confirmed that there are oxygenated species (Pt–OH_{ads} and/or Pt–O_{ads}) on the surface of platinum electrode,[22,23] which play an important role in the electrochemical reaction process. At 0.9 V, the oxide on the electrode surface was mainly OH_{ads}, as shown in Reaction R3. At 1.4 V, the oxide on the electrode surface was mainly O_{ads}, and its formation process was shown in Reaction R4.

$$[Pt] + H_2O \rightarrow [Pt]OH_{ads} + H^+ + e^- \quad (R3)$$

$$[Pt]OH_{ads} \rightarrow [Pt]O_{ads} + H^+ + e^- \quad (R4)$$

Figure 13 shows the changes in the concentrations of the surface species on the platinum electrode analyzed by on-line HPLC. The concentration of TU_2^{2+} on the electrode surface was increased during potential forward scanning. TU formed on the surface of the electrode during the forward scan. But the concentration of TU gradually decreases and reached a minimum value near 0.6 V. Simultaneously, the concentration of TU_2^{2+} on the electrode surface was gradually increased, reaching a maximum value at 0.6 V (Figure 13a), which corresponded to the oxidation peak near 0.6 V in Figure 11. Therefore, the oxidation peak of 0.6 V was related to the oxidation reaction of TU to form TU_2^{2+}, as shown in equations (R5) and (R6).

$$[Pt]OH_{ads} + (NH_2)_2CS - e^- \rightarrow [Pt][(NH_2)(NH)CSOH]_{ads} + H^+ \quad (R5)$$

$$[Pt][(NH_2)(NH)CSOH]_{ads} + (NH_2)_2CS + 2H^+ \rightleftharpoons [Pt] + [(NH_2)_2CSSC(NH_2)_2]^{2+} + H_2O \quad (R6)$$

TUO_2 was detected at 1.0 V during the forward scan (Figure 13c), which corresponded to the oxidation peak at 1.0 V in Figure 11. The process was owing to the oxidation of TU to TUO_2, as shown in equations (R7) and (R8). However, the concentration of TUO_2 on the electrode surface remained a stable value, and the concentration of TU_2^{2+} was decreased greatly from 1.0 V, which indicated that the TUO_2 originated from the oxidation of TU_2^{2+}, as shown in equation (R9). When the potential was reversed, the concentration of TU_2^{2+} on the electrode surface dropped sharply at 0.2 V (Figure 13d), whereas the concentration of TU significantly was increased (Figure 13e), corresponding to the cathodic peak of 0.2 V in Figure 11. This behavior indicated that TU_2^{2+} is reduced to TU at this potential, as shown in equation (R10). Additionally, the presence of TUO_2 was detected up to 0.8 V in the reverse scan, as shown in Figure 13f.

$$[Pt]O_{ads} + (NH_2)_2CS \rightarrow [Pt] + (NH_2)(NH)CSOH \quad (R7)$$

$$[Pt]O_{ads} + (NH_2)(NH)CSOH \rightarrow [Pt] + (NH_2)(NH)CSO_2H \quad (R8)$$

$$2[Pt]O_{ads} + [(NH_2)_2CSSC(NH_2)_2]^{2+} \rightarrow 2[Pt] + (NH_2)(NH)CSO_2H + NH_2CN + 2H^+ \quad (R9)$$

$$[Pt][(NH_2)_2CSSC(NH_2)_2]^{2+}_{ads} + 2e^- \rightarrow [Pt] + 2(NH_2)_2CS \quad (R10)$$

TU partially adsorbed on the surface of the platinum electrode may undergo platinum-catalyzed electrochemical reactions, such as oxidation to cyanamide (NH_2CN) and elemental sulfur (S),[24] as shown in equation (R11). Cyanamide cannot be detected quantitatively by HPLC because of its weak ultraviolet absorption. TU_2^{2+} hydrolyzed to TU, cyanamide, and elemental sulfur[25,26] were involved in equation (R12). Adsorbed cyanamide and elemental sulfur can be oxidized to carbon dioxide, nitrogen, and sulfate,[27,28] as shown in equations (R13) and (R14). These equations provided a plausible explanation for the complex behavior in the electro-oxidation of TU_2^{2+} in forced convection environment.

$$[Pt]((NH_2)_2CS)_{ads} \rightleftharpoons [Pt] + NH_2CN + S + 2H^+ + 2e^- \quad (R11)$$

$$[(NH_2)_2CSSC(NH_2)_2]^{2+}_{ads} \rightarrow NH_2CN + S + (NH_2)_2CS + 2H^+ \quad (R12)$$

$$[Pt](NH_2CN)_{ads} + 2H_2O \rightarrow [Pt] + CO_2 + N_2 + 6H^+ + 6e^- \quad (R13)$$

$$[Pt](S)_{ads} + 4H_2O \rightarrow [Pt] + SO_4^{2-} + 8H^+ + 6e^- \quad (R14)$$

3. Conclusion

Combining voltammetry with on-line HPLC technique, we provided an effective approach for the quantitative and qualitative determinations of electrode surface species. Using a microporous sampler on the platinum electrode surface, forced convection was induced by sampling and strengthened the mass transfer process on electrode surface, which promoted the renewal of the species involved in the reaction and further affected the redox peak currents. Kinetic information can be obtained through the change of the concentration of the species on the electrode surface along by the change of the electrode potential. As exemplified by the qualitative and quantitative analysis of the electro-oxidation products of TU_2^{2+}, this method allowed in situ detection of the species and concentration changes on the electrode surface. The main electro-oxidation products of TU_2^{2+} were found to be thiourea, TUO_2, cyanamide, and elemental sulfur. The results indicate that combining voltammetry with on-line HPLC technique would be an effective way to study the kinetics and mechanism of electro-oxidation of TU_2^{2+}. This work may open a new door for exploring complex electrochemical reactions on the electrode surface.

Experimental Section

All solutions were prepared using deionized Milli-Q water and analytical grade reagents. The reaction was carried out in a cylindrical glass electrochemical cell with a volume of approximately 80 mL, where TU_2^{2+} solution was filled at desired concentrations. The working electrode was a polycrystalline disk platinum electrode with a diameter of 5 mm. The auxiliary electrode was a thin platinum sheet (10×10×0.2 mm) and a saturated calomel electrode (SCE) was used as the reference electrode. All potentials in the experiments were referenced to the SCE. The electrolyte solution was 0.1 M perchloric acid. The reaction temperature was controlled using a circulating water bath (25±0.1 °C, Polyscience). A micro-sized sample collection tip (inner diameter of 0.3 mm) was fixed on the surface of the working electrode and the samples were collected online with a peristaltic pump (ISMATEC 78001-02) at different sampling rates during cyclic voltammetry measurements and analyzed by HPLC (Agilent 1260 LC) using a Phenomenex Ginimi C18 column (250×4.6 mm, 5 μm). The detector type was DAD (G4212B), and the detection wavelength was 195 nm, 214 nm, 235 nm and 254 nm, respectively. A schematic diagram of this device can be found in a previous paper.[9] For HPLC analysis, the mobile phase consisted of a mixture of methanol, acetonitrile, and 0.01 M hydrochloric acid (6:26:68, vol%). All the electrochemical experiments were carried out with a VSP-300 electrochemical station (BioLogic).

Acknowledgements

This work was supported by the Research Foundation Project of Zaozhuang University (No. 2017YB24), University Student Innovation and Entrepreneurship Training Scheme of Shandong Province (No. 202010904018), and the Doctoral Foundation Program of Zaozhuang University (No. 2019BS022, 2018BS060).

Conflict of Interest

The authors declare no conflict of interest.

Keywords: formamidine disulfide · electro-oxidation reactions · forced convection · HPLC · platinum electrodes

[1] A. Gherrou, H. Kerdjoudj, *Desalination* **2003**, *158*(1), 195–200.
[2] L. Vázquez, R. C. Salvarezza, A. J. Arvia, *Phys. Rev. Lett.* **1997**, *79*(4), 709–712.
[3] L. Wang, Z. Chen, M. Zhao, Y. Jin, *J. Mol. Catal.* **2018**, *32*(2), 187–193.
[4] T. S. Jagodziński, *Chem. Rev.* **2003**, *103*(1), 197–228.
[5] S. Wang, Q. Gao, J. Wang, *J. Phys. Chem. B* **2005**, *109*(36), 17281.
[6] S. V. Makarov, C. Mundoma, J. H. Penn, J. L. Petersen, S. A. Svarovsky, R. H. Simoyi, *Inorg. Chim. Acta* **1999**, *286*(2), 149–154.
[7] I. Lengyel, L. Gyorgyi, I. R. Epstein, *J. Phys. Chem.* **1995**, *99*(34), 12804–12808.
[8] G. Rábai, R. T. Wang, K. Kustin, *Int. J. Chem. Kinet.* **1993**, *25*, 53–62.
[9] W. Zhang, Y. Liu, H. Luo, B. Zhang, C. Pan, L. Zhang, *J. Electrochem. Soc.* **2019**, *166*, H736-H742.
[10] W. Cheuquepán, J. M. Orts, A. Rodes, *J. Electroanal. Chem.* **2016**, *764*, 79–87.
[11] V. Francisco, L. Garcia-Rio, J. A. Moreira, G. Stedman, *New J. Chem.* **2008**, *32*, 2292–2298.
[12] A. E. Bolzán, I. B. Wakenge, R. C. Salvarezza, A. J. Arvia, *J. Electroanal. Chem.* **1999**, *475*, 181–189.
[13] G. Garcia, J. L. Rodriguez, G. I. Lacconi, E. Pastor, *J. Electroanal. Chem.* **2006**, *588*(2),169–178.
[14] W. Cheuquepán, J.M Pérez, J. M. Orts, A. Rodes, *J. Phys. Chem. C* **2014**, *118*(33), 19070–19084.
[15] Y. Kwon, M. T. M. Koper, *Anal. Chem.* **2010**, *82*, 5420–5424.
[16] A. Santasalo-Aarnio, Y. Kwon, E. Ahlberg, K. Kontturi, T. Kallio, M. T. M. Koper, *Electrochem. Commun.* **2011**, *13*(5), 466–469.
[17] W. Zhang, C. Pan, Q. Gao, *J. Phys. Chem. C* **2018**, *122*, 24150–24157.
[18] D. Wielend, H. Neugebauer, N. S. Sariciftci, *Electrochem. Commun.* **2021**, *125*, 106998.
[19] A. Dushina, H. Schmies, D. Schonvogel, A. Dyck, P. Wagner, *Int. J. Hydrogen Energy* **2020**, *45*(60), 35073–35084.
[20] A. G. Zelinsky, *Electrochim. Acta* **2015**, *154*, 315–320.
[21] O. Azzaroni, G. Andreasen, B. Blum, R. C. Salvarezza, A. J. Arvia, *J. Phys. Chem. B* **2000**, *104*(7), 1395–1398.
[22] H. Imai, K. Izumi, M. Matsumoto, Y. Kubo, K. Kato, Y. Imai, *J. Am. Chem. Soc.* **2009**, *131*(17), 6293–6300.
[23] Y. Liu, A. Barbour, V. Komanicky, H. You, *J. Phys. Chem. C* **2016**, *120*(29), 16174–16178.
[24] G. García, J. L. Rodríguez, G. I. Lacconi, E. Pastor, *Langmuir* **2004**, *20*(20), 8773–8780.
[25] M. Yan, K. Liu, Z. Jiang, *J. Electroanal. Chem.* **1996**, *408*(1-2), 225–229.
[26] M. Hoffmann, J. O. Edwards, *Inorg. Chem.* **1978**, *16*(12), 3333–3338.
[27] A. E. Bolzán, P. L. Schilardi, R. C. V. Piatti, T. Iwasita, A. Cuesta, C. Gutiérrez, A. J. Arvia, *J. Electroanal. Chem.* **2004**, *571*(1), 59–72.
[28] G. García, J. L. Rodríguez, G. I. Lacconi, E. Pastor, *J. Electroanal. Chem.* **2006**, *588*, 169–178.

Manuscript received: August 24, 2021
Revised manuscript received: October 5, 2021